THE JOURNAL OF PHYSICAL CHEMISTRY LETTERS
A JOURNAL OF THE AMERICAN CHEMICAL SOCIETY

pubs.acs.org/JPCL
Letter

How to Probe Hydrated Dielectrons Experimentally: *Ab Initio* Simulations of the Absorption Spectra of Aqueous Dielectrons, Electron Pairs, and Hydride

Kenneth J. Mei, William R. Borrelli, José L. Guardado Sandoval, and Benjamin J. Schwartz*

Cite This: *J. Phys. Chem. Lett.* 2024, 15, 9557−9565
Read Online
ACCESS | Metrics & More | Article Recommendations | Supporting Information

ABSTRACT: In the radiation chemistry of water, two hydrated electrons (e^-_{hyd}) can react to form H_2 and OH^-. Experiments and simulations suggest that this reaction occurs through a mechanism involving colocalization of two e^-_{hyd}'s into the same solvent cavity, forming a hydrated dielectron ($(e_{hyd})_2^{2-}$) intermediate, with aqueous hydride (H^-) as a subintermediate. However, there has been no direct experimental observation of either $(e_{hyd})_2^{2-}$ or H^-. Here, we present TD-DFT-based predictions for the absorption spectrum of open-shell-singlet and triplet e^-_{hyd} pairs, $(e_{hyd})_2^{2-}$, and H^-. We find that relative to e^-_{hyd}, triplet and open-shell singlet electron pairs show spectral shifts to the blue and red, respectively. Additionally, we find that $(e_{hyd})_2^{2-}$ absorbs even further to the red, and that H^- has a charge-transfer-to-solvent-like transition at wavelengths several eV to the blue, providing a direct experimental handle with which to probe these species. We propose a three-pulse transient absorption experiment that should allow detection of $(e_{hyd})_2^{2-}$ and H^-.

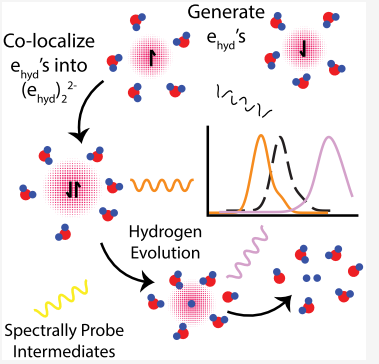

An excess electron in liquid water forms a stably solvated species known as the hydrated electron (e^-_{hyd}).[1−5] Though hydrated electrons are the simplest chemical solute, they display a wide array of fascinating properties and have been of considerable experimental[4−7] and theoretical[8−13] interest over the last several decades. Experimentally, hydrated electrons are easily made via pulse radiolysis,[4,5,14] multiphoton ionization,[15−18] or the charge-transfer-to-solvent excitation of solvated anions.[19−22] Theoretically, their treatment results in a challenging but potentially tractable quantum many-body problem.[23,24] Despite this, there are still many open questions about the e^-_{hyd}, namely the nature of the solvation structure around this species[8,9,25,26] and how the solvation structure controls its reactivity as a strong reducing agent in solution.[13,27−29]

Hydrated electrons are known to react with a variety of organic molecules,[30] and recent *ab initio* simulation work has illuminated some features of this reactivity,[13,28,29] particularly for the reduction of CO_2.[13,29] The reaction of interest for this work, which is common in the radiation chemistry of water, involves two hydrated electrons reacting with H_2O to form hydrogen gas and hydroxide:

$$e^-_{hyd} + e^-_{hyd} + 2H_2O \rightarrow H_2 + 2OH^- \quad (1)$$

This hydrogen evolution reaction typically takes place in high concentration e^-_{hyd} solutions. These solutions are thought to contain a mixture of single e^-_{hyd}'s, separate but spin-correlated e^-_{hyd} pairs with parallel spins (triplet), and separate but spin-correlated e^-_{hyd} pairs with opposite spins (open-shell singlet). It is also possible that two e^-_{hyd}'s at high concentration can occupy the same cavity in the singlet spin state, a species termed the hydrated dielectron, $(e_{hyd})_2^{2-}$.

Experiments have observed that atomic hydrogen is not a product of reaction (1) and that the only products are diamagnetic,[31] suggesting that H· is also not a reactive intermediate. Since triplet H_2 is unbound, the hydrated electrons that participate in this reaction, as well as any reactive intermediates, must be spin singlet.[31] Thus, the intermediates in this reaction have been speculated to be the spin-paired hydrated dielectron and/or the aqueous hydride ion.[32] From experimental measurements of the reaction rate, Schmidt and Bartels estimated that e^-_{hyd}'s within ∼9 Å of each other combine to initiate reaction (1).[31] The mechanism of this reaction is thought to proceed via the following multistep process involving formation of the $(e_{hyd})_2^{2-}$ intermediate:[33,34]

$$e^-_{hyd} + e^-_{hyd} \rightarrow +(e_{hyd})_2^{2-} \quad (2)$$

Received: August 15, 2024
Revised: September 5, 2024
Accepted: September 9, 2024
Published: September 12, 2024

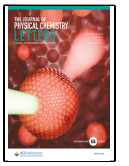

$$(e_{hyd})_2^{2-} + H_2O \rightarrow H^- + OH^- \quad (3)$$

$$H^- + H_2O \rightarrow H_2 + OH^- \quad (4)$$

Despite their potential importance as intermediates in reaction (1), the existence of hydrated dielectrons has not been directly established. Experiments have sought to measure this species using absorption spectroscopy, and early work from Basco et al.[35] argued that the absorption of the $(e_{hyd})_2^{2-}$ should occur in the IR at wavelengths >700 nm. However, subsequent works either did not find an IR absorbing species,[36] assigned the dielectron absorption as occurring in the UV,[37] or concluded that there were no absorption signatures consistent with $(e_{hyd})_2^{2-}$.[32] In alkali metal/ammonia solutions, dielectrons are suspected to play a role in the increased electrical conductivity and decreased spin density that accompany an insulator-to-metal transition observed with increasing alkali metal concentration.[38] Moreover, in recent work, Hartweg et al.[39] implicated the formation of dielectrons in ammonia clusters following UV excitation in the presence of already-existing solvated electrons.

Based on all the indirect experimental evidence for solvated dielectrons, there has been a significant theoretical push to understand their properties,[40−45] including previous work from our group.[33,46−48] *Ab initio* simulations predict that spin singlet hydrated electron pairs in close proximity preferentially occupy the same cavity,[33,34,49] forming $(e_{hyd})_2^{2-}$, and that spin triplet hydrated electron pairs prefer to occupy separate cavities.[34] All of the *ab initio* simulations,[34,49] including ours,[33] predict that hydrated dielectrons are indeed the primary intermediate of reaction (1), as specified in reactions (2) and (3).

Our previous publication studying reactions (2−4) found a range of lifetimes for the $(e_{hyd})_2^{2-}$ and H^- intermediates. We saw that a second electron injected in the presence of an already-equilibrated e_{hyd}^- instantaneously localizes into the same cavity to form $(e_{hyd})_2^{2-}$, giving a rigorous time zero for starting reaction (2). The $(e_{hyd})_2^{2-}$ lives for hundreds of femtoseconds, on average, before reaction (3) takes place.[33] We found that the time scale of this first proton abstraction to form H^- depends on the existence of a hydrogen bond network to shuttle the OH^- far from the reaction center through a Grotthus-type[50,51] proton hopping mechanism.[33] Once formed, the H^- intermediate exists for 10 to ∼150 fs, depending on the degree of solvation, before reaction (4) takes place.[33] These relatively short lifetimes are the reason why direct experimental detection of $(e_{hyd})_2^{2-}$ and H^- in reactions that require diffusion of two electrons to start reaction (2) has been unsuccessful thus far.

In this work, we propose that for the possible intermediates for reaction (1)—separated spin-paired singlet or triplet hydrated electron pairs, hydrated dielectrons in a single cavity and solvated H^-—the best route to investigate them experimentally is through ultrafast transient absorption spectroscopy.

To date, the only studies of hydrated dielectron spectroscopy via simulation was in previous work from our group using mixed quantum/classical simulations;[46−48] there have been no *ab initio*-based spectroscopic studies of paired hydrated electrons, dielectrons or H^-. If the absorption spectrum of $(e_{hyd})_2^{2-}$ (i.e., two spin singlet electrons localized to the same solvated cavity) has unique spectral features or dynamic behavior compared to that of a (single) e_{hyd}^-, then it should be possible to experimentally characterize this species if one knew where to look. It is also possible that as two hydrated electrons approach each other en route to reaction (2), their mutual coulomb repulsion and/or interaction of their solvation structures could affect their spectroscopy in measurable ways. The H^- intermediate in reaction (3) could also have experimentally identifiable spectral features.

The goal of this paper is to provide *ab initio*-predicted spectral features for all of these species, with the hope of inspiring experimentalists to look for their signatures. We take advantage of trajectories from our previous work[33] to perform a time-dependent density functional theory (TD-DFT) analysis of the spectroscopy of $(e_{hyd})_2^{2-}$ and H^-. We also study the spectral behavior of separate but interacting (single) e_{hyd}^- pairs in both the triplet and open-shell singlet spin states. We find that the absorption spectra of both triplet and open-shell singlet e_{hyd}^- pairs show noticeable shifts (∼0.2 eV) depending on the distance between them. As the distance between the electrons decreases, the absorption spectrum of open-shell singlet e_{hyd}^- pairs red-shifts, while that of spin triplet electron pairs blue-shifts, providing a definitive spectral signature of e_{hyd}^- interaction that could be observed experimentally. We also predict that if a second (opposite spin) hydrated electron is injected in the presence of an already-equilibrated e_{hyd}^-, dielectrons will be formed immediately, with a spectrum that is ∼0.3 eV red-shifted from that of the single e_{hyd}^-. Additionally, we predict that the H^- subintermediate has an absorption spectrum that is a few eV blue-shifted from all the other species, providing a unique spectral window for its potential observation. With knowledge of the spectroscopy and lifetimes of the reaction (1) intermediates,[33] we offer a set of specific pump/probe experiments that could be performed to detect these species.

The details of our simulations are largely the same as those used in our previous work[9] and are described in more detail below in the Methods section. Briefly, we perform AIMD simulations with 64 water molecules and one or two excess electrons in the *N*, *V*, *T* ensemble at 298 K. The PBE0[52] exchange-correlation functional was used with 25% exact exchange with Grimme's D3 dispersion correction.[53] In this work, hydrated (di)electrons are represented using their maximally localized Wannier functions (MLWFs),[54] and their positions determined as the Wannier orbital centers (WOCs).

Sixteen trajectories were performed in which a second e_{hyd}^- was injected into an already equilibrated e_{hyd}^- system with parallel spins to simulate triplet e_{hyd}^- pairs. We then took 22 equilibrated triplet electron pair congifurations and changed the spin state to antiparallel, thus simulating open-shell singlet e_{hyd}^- pairs. The open-shell singlet systems were run until the e_{hyd}^- pairs recombined into hydrated dielectrons, which occurred in less than 1.5 ps in 13 of our trajectories. Configurations for calculating the spectra of $(e_{hyd})_2^{2-}$ and H^- were taken from trajectories from our previous work.[33] These $(e_{hyd})_2^{2-}$ configurations were pulled from trajectories a few hundred fs after injection of the second e_{hyd}^- to provide time for solvent equilibration, and also were sampled prior to the start of reaction (3). Hydride configurations were taken after the completion of reaction (3) and prior to the start of reaction (4).

https://doi.org/10.1021/acs.jpclett.4c02404
J. Phys. Chem. Lett. 2024, 15, 9557−9565

Absorption spectra were calculated using Tamm-Dancoff approximation (TDA) TD-DFT in CP2K.[55] These calculations are fully periodic and 10 excited states were used to determine the spectra for e^-_{hyd}/paired e^-_{hyd} systems, while 20 excited states were used for the $(e_{hyd})_2^{2-}$ and H^- systems. We note that use of this methodology introduces a significant spectral blue-shift compared to both our previous nonperiodic calculations that used an optimally tuned range-separated hybrid functional[9,11,56] and the experimental spectrum.[57] This methodology is also known to sometimes include spurious charge transfer transitions,[9,58] and these are removed from our spectra using the so-called "Ghost Hunter" index.[59] Further details can be found in the Methods section and SI. However, use of the periodic TD-DFT methodology does allow us to make rigorous relative spectral comparisons between each of the electron-based species explored in this work. Further details on calculation of the absorption spectra are provided in the Methods section.

To understand the spectral features of the intermediates associated with reaction (1), we start by examining what happens when hydrated electrons are present in close proximity (i.e., the left side of reaction (2)). Previous experiments have initiated reaction (2) through the generation of high-concentration e^-_{hyd} solutions via either pulse radiolysis[31,32] or flash photolysis.[35,37] It is thought that singlet e^-_{hyd} pairs can combine via diffusion to form $(e_{hyd})_2^{2-}$, while triplet e^-_{hyd} pairs cannot form dielectrons.[31] The questions we now address pertaining to reaction (2) are: do spin-correlated e^-_{hyd} pairs have spectral features that are distinct from those of the equilibrium hydrated electrons? Is there any difference between the absorption spectra of singlet and triplet e^-_{hyd} pairs?

In Figures 1b and d, respectively, we report the electron−electron distance ($r_{1,2}$, calculated as the distance between WOCs) dependent absorption spectra of triplet (blue curves) and open-shell singlet (green curves) e^-_{hyd} pairs. The black dashed line in each panel marks the peak of the equilibrium absorption spectrum of the (single) e^-_{hyd} calculated using the same methodology. At relatively far distances ($r_{1,2} \geq 5.7$ Å), the spectra of triplet and open-shell singlet e^-_{hyd} pairs matches that of single hydrated electrons; the electron pairs also have similar solvation structures as single hydrated electrons (Figure S5 in the SI). As $r_{1,2}$ decreases, however, we observe significant (~0.2 eV) shifts of the spectra of triplet and open-shell singlet electron pairs: the spectrum blue-shifts as triplet-paired electrons approach each other, but red-shifts when the electrons' spin are open-shell singlet.

Spectroscopically, hydrated electrons behave roughly as particles in a spherical box, with three quasi-degenerate $s \rightarrow p$ electronic transitions.[60] Indeed, visualization using natural transition orbitals[61] (Figure S6 in the SI) show that our TD-DFT-calculated spectral transitions do resemble $s \rightarrow p$ transitions. In the spherical box model, the excitation energies depend on the size of the box, which for a e^-_{hyd} is roughly its radius of gyration (R_g). Figures 1a and c show scatter plots of the average radius of gyration, $\langle R_g \rangle$, calculated from the MLWFs of both electrons, versus $r_{1,2}$ for triplet and open-shell singlet electron pairs, respectively. The solid black lines are least-squares fits to the data points to emphasize the trends. Clearly, the $\langle R_g \rangle$ of triplet e^-_{hyd} pairs decreases and that of open-shell singlet e^-_{hyd} pairs increases as the electrons approach each other. This trend correlates well with the observed spectral shifts, with smaller box sizes for triplet pairs increasing the excitation energies while larger box sizes for singlet pairs decrease excitation energies as the electrons get closer to each other.

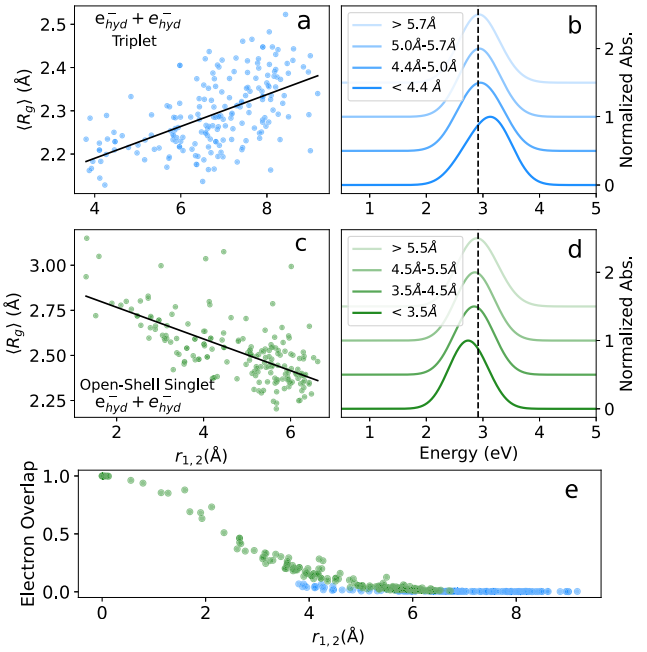

Figure 1. Comparison of the average radius of gyration, $\langle R_g \rangle$, panels (a) and (c), and the TD-DFT-calculated absorption spectra, panels (b) and (d), as a function of the electron−electron distance, ($r_{1,2}$), for triplet and open-shell singlet hydrated electron pairs, respectively. The black lines in panels (a) and (c) are least-squares fits to the data points to emphasize the trends. The $\langle R_g \rangle$ of triplet electron pairs decreases as the electrons approach each other while that of open-shell singlet electron pairs increases. This leads to a blue-shift of the spectrum of triplet pairs and a red-shift of that of open-shell singlet pairs relative to the spectrum of (single) hydrated electrons, whose spectral maximum is indicated by the black dashed lines in panels (b) and (d). Panel (e) plots the electron−electron MLWF overlap for both types of electron pairs as a function of $r_{1,2}$. When in close proximity, open-shell singlet electron pairs (green data points) are able to overlap while triplet pairs (blue data points) are not, explaining the observed trends in $\langle R_g \rangle$.

The fact that singlet and triplet e^-_{hyd} pairs have opposite spectral trends with distance is likely due to Pauli repulsion. As the e^-_{hyd} cavities become closer together, the parallel spins of triplet e^-_{hyd} pairs prevent the two electrons from overlapping in space. This Pauli repulsion causes each e^-_{hyd} to decrease its R_g to accommodate the proximity of the other electron. For open-shell singlet pairs, in contrast, electrons with opposite spin can overlap in close proximity; this means that each electron can slightly occupy the other's cavity, increasing their $\langle R_g \rangle$. Figure 1e plots the electron−electron overlap for triplet (blue data points) and open-shell singlet (green data points) e^-_{hyd} pairs, calculated as the dot product of their MLWF densities. The data show that the open-shell singlet electron−electron overlap increases with decreasing $r_{1,2}$ while the triplet electron−electron overlap remains close to zero as the electrons approach each other, consistent with the distance-dependent trends in $\langle R_g \rangle$. Additionally, the absence of configurations with closer $r_{1,2}$ highlights the significant energetic barrier for triplet e^-_{hyd} pairs to spatially overlap.

The data in Figure 1 predict that there is a distinct spectral feature associated with the recombination of singlet e^-_{hyd} pairs

https://doi.org/10.1021/acs.jpclett.4c02404
J. Phys. Chem. Lett. 2024, 15, 9557−9565

that may be detectable via transient absorption spectroscopy. One possible experiment would be to generate a high concentration of e^-_{hyd}'s via some short-pulse method, such as pulse radiolysis,[31,32] charge-transfer-to-solvent excitation of a dissolved anion like I^- or $[Fe(CN)_6]^{4-}$,[19−22] or direct multiphoton ionization of water.[15−18] It is well-known that following their initial injection, nonequilibrated hydrated electrons absorb to the red of the equilibrium e^-_{hyd} spectrum, but equilibration is known to be complete in ≤1 ps after injection.[20,62−64] Once equilibrated, if the concentration is high enough, a subset of the electrons will be paired as open-shell singlets, producing a red shoulder in the transient absorption spectrum that should decay on the time scale of reaction (2), leaving the equilibrium (single) e^-_{hyd} spectrum behind. It might also be possible to pick up the spectral signatures of proximal triplet e^-_{hyd} pairs (for which there should be three times as many as singlet pairs given the spin statistics) as a blue shoulder on the equilibrium spectrum, although this may be harder to detect given that the equilibrium spectrum has a strong absorption tail to the blue.[57]

It is worth noting, however, that our simulations predict a significant absorption spectral shift only at quite small electron−electron distances. If the paired hydrated electrons are separated by ≥6 Å, their spectra are indistinguishable from those of equilibrated single hydrated electrons. If the reaction distance of ∼9 Å estimated for reaction (2) is correct,[31] then there would be very little transient population of singlet e^-_{hyd} pairs relative to single hydrated electrons, thus decreasing the chance of detecting this species via transient absorption spectroscopy.

Given the challenges in measuring the spectral shifts of hydrated electron pairs at high concentrations, we next propose a different experiment[46−48] that should provide better access to detect the presence of the $(e_{hyd})^{2-}_2$ and possibly also the H^- reactive intermediates. First, a short laser or radiolysis pulse could be used to generate hydrated electrons. After a time delay to ensure that this population reaches equilibrium, a second pulse could then used to generate additional electrons; based on our previous simulations,[33] some of these will colocalize into the same cavity as a pre-equilibrated hydrated electron, directly creating $(e_{hyd})^{2-}_2$. The second pulse thus provides a rigorous time zero for the generation of a $(e_{hyd})^{2-}_2$ population, which is expected to live for ∼1 ps.[33] The questions we explore next is what are the spectral features of the dielectron, and is there is an experiment that could also detect the H^- subintermediate?

Figure 2 plots radial distribution functions (RDFs) between the centers of the electron (black dashed curves), dielectron (orange curves) and the H (panel a) or O (panel b) atoms of the surrounding water molecules; panel c shows running coordination numbers calculated by integrating the center-to-oxygen RDFs. The data show that the hydrated dielectron has a slightly larger cavity than the (single) e^-_{hyd}, as seen from the fact that its first shell peaks sit at a farther distance. The running coordination number shows that the larger and more highly charged $(e_{hyd})^{2-}_2$ has an additional coordinating water molecule (∼6) compared to the single e^-_{hyd} (∼5).[10] We also find an R_g of 2.91 Å for $(e_{hyd})^{2-}_2$ compared to 2.51 Å for the single e^-_{hyd}, as calculated using their MWLF densities. All of these measures indicate that the hydrated dielectron sits in a

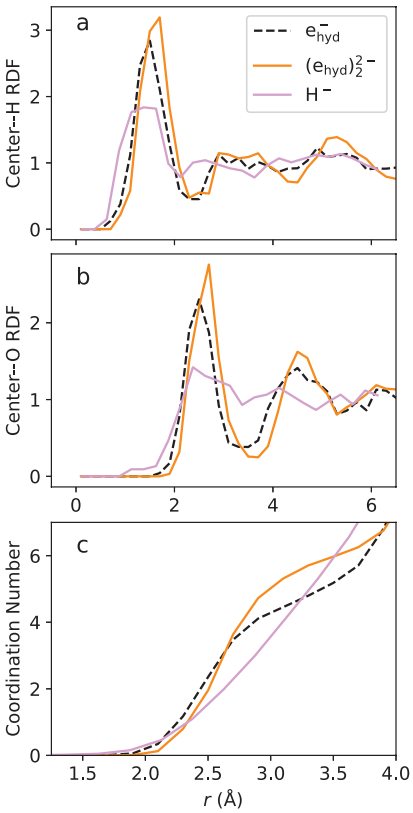

Figure 2. Radial distribution functions (RDFs) of the hydrated electron, hydrated dielectron, and hydride from our DFT-based simulations. Panel a shows center to water H RDFs, panel b shows center to water O RDFs, and panel c shows the running water coordination number of each species. The black dashed, orange, and plum curves correspond to the hydrated electron, hydrated dielectron, and hydride, respectively. The positions of the first-shell H and O atoms are slightly farther for dielectrons than for (single) hydrated electrons, indicating a larger cavity. The running coordination number shows that the larger dielectron has ∼6 first-shell waters, which is more than the ∼5 of the single hydrated electron. Since hydride is generated when the dielectron abstracts a proton from a coordinating water and does not have time to equilibrate, the H^- solvation structure is similar to that of the dielectron water structure, though perturbed.

larger cavity than the hydrated electron, which along with the electron−electron repulsion should give a distinct spectral signature that could be detected by transient absorption.

Figure 2 also shows the solvation structure of the H^- subintermediate (plum curves). Our previous simulations indicate that H^- lives for ≤100 fs due to the rapid rate of reaction (4),[33] so the solvent structure of this species never fully comes to equilibrium before it reacts. As a result, H^- largely adopts the solvation structure left behind by the $(e_{hyd})^{2-}_2$ that created it from reaction (3), so the two species have generally similar RDFs. We note that H^- is significantly smaller than the dielectron due to coulomb attraction from the central proton, which allows some of the first-shell waters to move closer to the H^- center prior to reaction (4), as seen by the tails toward smaller distances in the RDFs.

Figure 3 plots the TD-DFT calculated optical absorption spectra of the hydrated electron (black dashed curve), hydrated dielectron (orange curve), and hydride (plum curve). The $(e_{hyd})^{2-}_2$ spectrum exhibits a significant red-shift

https://doi.org/10.1021/acs.jpclett.4c02404
J. Phys. Chem. Lett. 2024, 15, 9557−9565

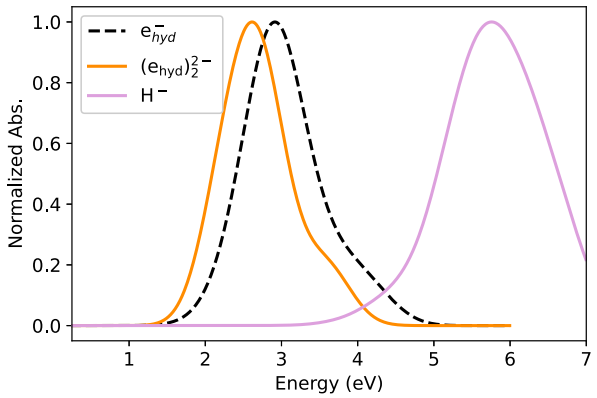

Figure 3. TD-DFT calculated and normalized absorption spectra of the hydrated electron (black dashed curve) and the hydrated dielectron (orange curve) and hydride (plum curve) reactive intermediates. Relative to the spectrum of the single e^-_{hyd}, the absorption spectrum of the dielectron intermediate shows a significant red-shift, providing a signature that could be detected experimentally. The hydride subintermediate exhibits a large spectral blue shift relative to the other species, offering another potential spectroscopic signature that could be used to test the mechanism of reaction (1).

of ∼0.3 eV compared to that of the single e^-_{hyd}. This red-shift results from both the fact that the dielectron has a larger cavity and thus R_g and the fact that the coulomb and exchange repulsion between the two electrons should raise the ground-state energy more than the excited-state energies relative to the (single) e^-_{hyd}. We note that the spectral shift is larger than that of the open-shell singlet e^-_{hyd} pair in close proximity due both to the larger R_g and the stronger coulomb/exchange repulsion of $(e_{hyd})^{2-}_2$ from greater electron overlap.

Our prediction is that if one were to create dielectrons with two sequential pump pulses to induce colocalization, a third probe pulse should be able to detect them by probing at wavelengths on the red side of the single e^-_{hyd} absorption spectrum. This prediction falls along the same lines as Basco et al.,[35] who also concluded that the signature absorption of the dielectron occurs in the IR at wavelengths >700 nm. The one caveat for this experiment is that the predicted lifetime of $(e_{hyd})^{2-}_2$ is comparable to the solvation relaxation time of the (single) electrons generated by the second pump pulse, so precise characterization of the solvation dynamics following the first pump pulse will be needed to determine if the second pump pulse produces an additional red-shifted spectral feature associated with dielectrons.

Our simulations also predict that even though the H^- subintermediate has a much shorter lifetime than $(e_{hyd})^{2-}_2$, it might be easier to detect spectroscopically: the plum curve in Figure 3 suggests that H^- absorbs several eV to the blue of hydrated electrons and dielectrons. In the gas phase, H^- does not have any bound electronic excited states,[65] but the presence of surrounding solvent can create bound excitations, referred to as charge-transfer-to-solvent (CTTS) states. The position of the H^- absorption band fits well to assignment as a CTTS transition. Previous calculations predicted that the CTTS spectrum of aqueous Na^- would be at ∼3 eV,[66] and one would expect the H^- CTTS excitation to be higher in energy than that of Na^- based on the higher electron affinity of H relative of Na. In the SI, we provide snapshots of the H^- NTOs associated with the strongly allowed TD-DFT transitions, which do somewhat resemble what might be expected for a CTTS transition.

In conclusion, we report predicted spectroscopic signatures of the reactive intermediates that take part in reaction (1). Direct measurements of open-shell singlet and triplet e^-_{hyd} pairs might be feasible in experiments generating high concentrations of e^-_{hyd} through short-pulse methods: open-shell singlet e^-_{hyd} pairs are predicted to exhibit a detectable red shoulder on the equilibrium e^-_{hyd} absorption spectrum, while triplet electron pairs in close proximity should exhibit a blue shoulder, leading to a potentially observable broadening of the spectrum relative to the spectrum of single hydrated electrons. For hydrated dielectrons, despite a large amount of theoretical interest, there has yet to be any direct observation by experiment. To remedy this, we have proposed the following three-pulse transient absorption experiment to detect this important intermediate.

The first pulse in this experiment is used to generate single hydrated electrons in solution. Techniques such as multiphoton ionization,[67,68] CTTS excitation of anions,[19−22] or pulse radiolysis[31] can generate high concentrations of injected hydrated electrons, in some cases up to decimolar concentrations.[67] These conduction band electrons are then allowed to equilibrate into hydrated electrons. This first set of hydrated electrons would have a half-life of up to microseconds,[69] providing ample time and trap density for the introduction of the secondary pulses for electron capture and subsequent probing.

Once the first population of hydrated electrons is equilibrated, a second set of hydrated electrons is then injected into the solution via one of the methods listed above. Our previous experiments have shown that injected electrons in aqueous NaCl solutions preferentially localize near Na^+ traps rather than localizing independently into cavities irrespective of traps.[70] Other experimental work that injected electrons at decimolar concentrations into liquid water observed saturation of the available traps, forcing these electrons to remain delocalized in the conduction band until additional traps became available.[67] These results suggest that injected electrons are always trap-seeking, and thus should prefer to localize in the cavities of pre-existing hydrated electrons rather than elsewhere in the liquid. Indeed, our previous theoretical work[33,46−48] has shown that injected electrons are captured with 100% efficiency if a previously equilibrated hydrated electron is available. Moreover, theoretical work by Bu and co-workers has shown that hydrated dielectrons are energetically more stable than two separate single hydrated electrons.[34] Together, this body of experimental and theoretical work suggests that equilibrated hydrated electrons, which can be produced in decimolar concentrations,[67] can serve as traps for injected conduction band electrons (if they are spin antiparallel).

One caveat with the source of the secondary injected conduction band electrons is that their introduction should not directly perturb the population of pre-existing electrons. For example, if one were to create the secondary electrons via multiphoton ionization at 266 nm,[67,68] some of the pre-existing electrons might also be excited at this wavelength, leading to signals that could confound the observation of dielectrons. However, hydrated electrons have a very low absorption cross-section at 266 nm,[3] and if one generated the secondary electrons via CTTS excitation of a strongly absorbing species like $K_4Fe(CN)_6$,[70,71] nearly all of the light would be absorbed

https://doi.org/10.1021/acs.jpclett.4c02404
J. Phys. Chem. Lett. 2024, 15, 9557−9565

by the ferrous cyanide with essentially no excitation of the pre-existing hydrated electrons.

Once the secondary electrons are injected, 25% of them should have singlet-paired spins with the pre-existing hydrated electrons; as argued above, the fact that hydrated electrons are trap-seeking suggests that a significant fraction of these should be captured by the pre-existing electrons to form dielectrons. The dielectrons have a unique spectral feature, absorbing well to the red of single hydrated electrons. Of course, the "hot" injected electrons that do not recombine into dielectrons will also absorb to the red of the single hydrated electron, but the spectral kinetics of hot electron relaxation have been well-studied since the 1980s.[20,62−64] In our proposed 3-pulse experiment, the spectral relaxation of "hot" single hydrated electrons can be well characterized after the first excitation pulse, so that one could look for spectral differences associated with the second excitation pulse that would be indicative of dielectron formation. Given that the lifetime of hydrated dielectrons in our simulations is predicted to be longer than the relaxation time of single injected electrons,[33] it should be possible to see the singlet hydrated dielectrons after any triplet-paired hydrated electrons and noncaptured singlet hydrated electrons have finished their relaxation process.

Spectral detection of hydrated dielectrons will be aided by the fact that their oscillator strength is twice that of single hydrated electrons, so that it may be possible to isolate their spectral signatures even if only a few percent of the secondary hydrated electrons are converted to dielectrons. If needed, one could also run the experiment at higher temperatures, where the rate of dielectron conversion to hydrogen slows down,[31,72] possibly extending the lifetime of this important reactive intermediate.

We also predict that the same 3-pulse experiment might be able to detect the hydride ion subintermediate by probing deep in the UV, providing possible proof of the mechanism suggested by reactions (3) and (4). We acknowledge that the hydride lifetime as characterized by our previous work[33,34] is short (order tens to ∼100 fs), however, the distinctness of its spectral signature relative to the other intermediates may make its detection feasible, albeit difficult.

METHODS

To simulate the hydrated dielectron via sequential injection of an excess electron into an already equilibrated single electron system,[33] we used starting configurations from our previously published single hydrated electron simulations.[9] These simulations were done with the CP2K[73] software package in the *N*, *V*, *T* ensemble at a temperature of 298 K. The simulation cell contained 64 water molecules with a cell length of 12.427 Å. A time step of 0.5 fs was used, and a Nose-Hoover[74] chain thermostat was coupled to the system to maintain the target temperature. The volume of the system was chosen to reproduce the experimental density of water at 298 K and 1 atm. The PBE0 exchange-correlation functional with default 25% exact exchange, Grimme's D3 dispersion correction,[53] and Goedecker-Teter-Hutter(GTH) pseudopotentials[75] along with the TZVP-GTH basis set were used in these simulations. Hartree−Fock (HF) exchange calculations were expedited by way of an auxiliary density matrix method.[76] We acknowledge that other groups have simulated the hydrated electron with the PBE0 functional using 40% exact exchange,[10,12] including work studying the DEHE reaction.[34] Our previous work has shown that the resulting solvation structure for 25% or 40% exact exchange PBE0 are nearly identical.[9] Moreover, the agreement of our current work with that of Bu and co-workers[34] indicates that, for the case of dielectron reactivity, varying the amount of exact exchange over this range does not make a significant difference.

Absorption spectra calculations were done using Tamm-Dancoff time-dependent density functional theory[55] (TD-DFT) in CP2K.[73] The calculations were fully periodic and for each configuration, 10 excited states were calculated for the e^-_{hyd} and paired e^-_{hyd} systems, while 20 excited states were used for the $(e_{hyd})^{2-}_2$ and H^- species. Approximately 50−100 configurations were used for each system.

Previously, we calculated the absorption spectrum of the (single) hydrated electron using a nonperiodic TD-DFT methodology suggested by Uhlig et al.,[77] which involves periodic replication of point charges around the quantum box, removal of periodic boundary conditions, and the use of an optimally tuned range-separated hybrid functional. Unfortunately, for the simulations presented here, the process of replication is complicated by the inclusion of two electrons that in many configurations exist relatively far apart. This led to difficulties with performing this replication because electrons near the edge of the simulation box did not remain localized in their cavities. Therefore, we decided to do fully periodic TD-DFT calculations to obtain the absorption spectra in this work. We note that this makes comparing the spectra presented here to those presented in previous work more difficult, but this choice allows for a detailed comparison of the spectra of the different intermediates that are calculated at the same level of theory.

As mentioned above, calculating the spectra using periodic TD-DFT calculations also leads to issues with spurious charge transfer states,[59,78,79] so to remedy this we employed the so-called ghost hunter index[59] to identify and remove such spurious states. We found that the only spurious states with non-negligible oscillator strengths appeared on the red-side of the calculated spectrum and that there were no nonspurious states in this region, so we also implemented an energy cutoff whereby transitions with energies below the cutoff were removed from our spectral calculations. Details of how we developed the cutoff are shown in the SI.

In our previous work,[9] where the single electron absorption spectra was calculated using the nonperiodic TD-DFT methodology of Uhlig et al.,[77] the peak of the absorption spectrum occurred at an energy of 2.52 eV, which is already significantly blue-shifted from the experimental absorption peak at 1.73 eV.[80] For the periodic TDA TD-DFT calculations of the single hydrated electron in this work, we find that the calculated peak is further blue-shifted by ∼0.4 eV, lying at 2.92 eV. This additional blue shift likely results from a combination of periodic boundary effects and the use of the PBE0 functional instead of the optimally tuned range-separated hybrid ω-PBE functional.

For the structural analyses used in this work, including the RDFs and calculation of R_g and $r_{1,2}$, maximally localized Wannier functions (MLWFs) were used to represent the hydrated electron(s). We used the Wannier orbital centers to determine of the positions and radii of gyration of the (di)electron(s). We note that this measure provides a slightly different center position than the spin density or SOMO that we explored in our previous work.[9] We made this choice because the spin density cannot be used for the hydrated

https://doi.org/10.1021/acs.jpclett.4c02404
J. Phys. Chem. Lett. 2024, 15, 9557−9565

dielectron or open-shell singlet electron pairs because both electrons occupy the same spatial orbital with opposite spins. A similar issue affects triplet electron pairs, whose Kohn−Sham orbitals are near-degenerate, so that each hydrated electron can partially occupy both cavities, leading to an artificially high R_g and skewing the calculated center to lie between the two cavities. Our choice to use MLWFs thus allowed us to analyze all the two-electron systems on the same theoretical footing. A comparison of R_g calculated using the spin density, SOMO and MLWF representations of the e^-_{hyd} can be seen in Figure S4 in the SI.

■ ASSOCIATED CONTENT

Data Availability Statement

Any data generated and analyzed for this study that are not included in this Article and its Supporting Information are available from the authors upon reasonable request. The computer code used in this study is available from the authors upon reasonable request.

Supporting Information

The Supporting Information is available free of charge at https://pubs.acs.org/doi/10.1021/acs.jpclett.4c02404.

Additional data on spurious charge transfer states, additional structural comparisons and snapshots of natural transition orbitals (PDF)

■ AUTHOR INFORMATION

Corresponding Author

Benjamin J. Schwartz − *Department of Chemistry & Biochemistry, University of California, Los Angeles, Los Angeles, California 90095-1569, United States;* orcid.org/0000-0003-3257-9152; Phone: (310) 206-4113; Email: schwartz@chem.ucla.edu

Authors

Kenneth J. Mei − *Department of Chemistry & Biochemistry, University of California, Los Angeles, Los Angeles, California 90095-1569, United States*

William R. Borrelli − *Department of Chemistry & Biochemistry, University of California, Los Angeles, Los Angeles, California 90095-1569, United States*

José L. Guardado Sandoval − *Department of Chemistry & Biochemistry, University of California, Los Angeles, Los Angeles, California 90095-1569, United States*

Complete contact information is available at: https://pubs.acs.org/10.1021/acs.jpclett.4c02404

Notes

The authors declare no competing financial interest.

■ ACKNOWLEDGMENTS

This work was supported by the National Science Foundation program under Grant CHE-2247583. We gratefully acknowledge the Institute for Digital Research and Education (IDRE) at UCLA for use of the Hoffman2 computing cluster and ACCESS under computational project TG-CHE230086.

■ REFERENCES

(1) Walker, D. C. The hydrated electron. *Quarterly Reviews, Chemical Society* **1967**, *21*, 79−108.

(2) Hart, E. J.; Anbar, M. *Hydrated electron*; John Wiley and Sons, Inc., 1970; pp 77−79.

(3) Hart, E. J.; Boag, J. W. Absorption spectrum of the hydrated electron in water and in aqueous solutions. *J. Am. Chem. Soc.* **1962**, *84*, 4090−4095.

(4) Gordon, S.; Hart, E. J.; Matheson, M. S.; Rabani, J.; Thomas, J. K. Reactions of the hydrated electron. *Discuss. Faraday Soc.* **1963**, *36*, 193−205.

(5) Hart, E. J. The Hydrated Electron. *Science* **1964**, *146*, 19−25.

(6) Anbar, M.; Alfassi, Z. B.; Bregman-Reisler, H. Hydrated Electron Reactions in View of Their Temperature Dependence. *J. Am. Chem. Soc.* **1967**, *89*, 1263−1264.

(7) Marin, T. W.; Takahashi, K.; Jonah, C. D.; Chemerisov, S. D.; Bartels, D. M. Recombination of the Hydrated Electron at High Temperature and Pressure in Hydrogenated Alkaline Water. *J. Phys. Chem. A* **2007**, *111*, 11540−11551.

(8) Borrelli, W. R.; Mei, K. J.; Park, S. J.; Schwartz, B. J. Partial Molar Solvation Volume of the Hydrated Electron Simulated Via DFT. *J. Phys. Chem. B* **2024**, *128*, 2425−2431.

(9) Park, S. J.; Schwartz, B. J. Understanding the Temperature Dependence and Finite Size Effects in Ab Initio MD Simulations of the Hydrated Electron. *J. Chem. Theory Comput.* **2022**, *18*, 4973−4982.

(10) Pizzochero, M.; Ambrosio, F.; Pasquarello, A. Picture of the wet electron: a localized transient state in liquid water. *Chemical Science* **2019**, *10*, 7442−7448.

(11) Park, S. J.; Schwartz, B. J. How Ions Break Local Symmetry: Simulations of Polarized Transient Hole Burning for Different Models of the Hydrated Electron in Contact Pairs with Na+. *J. Phys. Chem. Lett.* **2023**, *14*, 3014−3022.

(12) Lan, J.; Rybkin, V. V.; Pasquarello, A. Temperature Dependent Properties of the Aqueous Electron. *Angew. Chem., Int. Ed.* **2022**, *61*, No. e202209398.

(13) Rybkin, V. V. Mechanism of Aqueous Carbon Dioxide Reduction by the Solvated Electron. *J. Phys. Chem. B* **2020**, *124*, 10435−10441.

(14) Walker, D. C. The hydrated electron. *Quarterly Reviews, Chemical Society* **1967**, *21*, 79−108.

(15) Long, F. H.; Lu, H.; Shi, X.; Eisenthal, K. B. Intensity dependent geminate recombination in water. *Chemical physics letters* **1991**, *185*, 47−52.

(16) Madsen, D.; Thomsen, C. L.; Thøgersen, J.; Keiding, S. Temperature dependent relaxation and recombination dynamics of the hydrated electron. *J. Chem. Phys.* **2000**, *113*, 1126−1134.

(17) Laenen, R.; Roth, T.; Laubereau, A. Novel precursors of solvated electrons in water: evidence for a charge transfer process. *Physical review letters* **2000**, *85*, 50.

(18) Hirata, Y.; Mataga, N. Direct observation of electron-cation geminate pair produced by picosecond laser pulse excitation in nonpolar solvent: excitation wavelength dependence of the electron thermalization length. *J. Phys. Chem.* **1991**, *95*, 1640−1644.

(19) Martini, I. B.; Barthel, E. R.; Schwartz, B. J. Mechanisms of the ultrafast production and recombination of solvated electrons in weakly polar fluids: Comparison of multiphoton ionization and detachment via the charge-transfer-to-solvent transition of Na in THF. *J. Chem. Phys.* **2000**, *113*, 11245−11257.

(20) Kee, T. W.; Son, D. H.; Kambhampati, P.; Barbara, P. F. A unified electron transfer model for the different precursors and excited states of the hydrated electron. *J. Phys. Chem. A* **2001**, *105*, 8434−8439.

(21) Gelabert, H.; Gauduel, Y. Short-Time Electron Transfer Processes in Ionic Aqueous Solution: Counterion and H/D Isotope Effects on Electron- Atom Pairs Relaxation. *J. Phys. Chem.* **1996**, *100*, 13993−14004.

(22) Vilchiz, V. H.; Kloepfer, J. A.; Germaine, A. C.; Lenchenkov, V. A.; Bradforth, S. E. Map for the relaxation dynamics of hot photoelectrons injected into liquid water via anion threshold photodetachment and above threshold solvent ionization. *J. Phys. Chem. A* **2001**, *105*, 1711−1723.

(23) Rossky, P. J.; Schnitker, J. The hydrated electron: quantum simulation of structure, spectroscopy, and dynamics. *J. Phys. Chem.* **1988**, *92*, 4277−4285.
(24) Turi, L.; Rossky, P. J. Theoretical Studies of Spectroscopy and Dynamics of Hydrated Electrons. *Chem. Rev.* **2012**, *112*, 5641−5674.
(25) Turi, L.; Borgis, D. Analytical investigations of an electron−water molecule pseudopotential. II. Development of a new pair potential and molecular dynamics simulations. *J. Chem. Phys.* **2002**, *117*, 6186−6195.
(26) Glover, W. J.; Schwartz, B. J. Short-range electron correlation stabilizes noncavity solvation of the hydrated electron. *J. Chem. Theory Comput.* **2016**, *12*, 5117−5131.
(27) Liu, P.; Zhao, J.; Liu, J.; Zhang, M.; Bu, Y. Ab initio molecular dynamics simulations reveal localization and time evolution dynamics of an excess electron in heterogeneous CO2−H2O systems. *J. Chem. Phys.* **2014**, *140*, 044318.
(28) Renault, J. P.; Pommeret, S. Seeing the solvated electron in action: First-principles molecular dynamics of NO3- and N2O reduction. *Radiat. Phys. Chem.* **2022**, *190*, 109810.
(29) Neupane, P.; Bartels, D. M.; Thompson, W. H. Exploring the Unusual Reactivity of the Hydrated Electron with CO2. *J. Phys. Chem. B* **2024**, *128*, 567−575.
(30) Daily, R.; Minakata, D. Reactivities of hydrated electrons with organic compounds in aqueous-phase advanced reduction processes. *Environmental Science: Water Research & Technology* **2022**, *8*, 543−574.
(31) Schmidt, K.; Bartels, D. Lack of ionic strength effect in the recombination of hydrated electrons:(e-) aq+(e-) aq → 2 (OH-)+ H2. *Chemical physics* **1995**, *190*, 145−152.
(32) Meisel, D.; Czapski, G.; Matheson, M. S.; Mulac, W. On the existence of dielectrons in aqueous solutions. *International Journal for Radiation Physics and Chemistry* **1975**, *7*, 233−241.
(33) Borrelli, W. R.; Guardado Sandoval, J. L.; Mei, K. J.; Schwartz, B. J. Roles of H-Bonding and Hydride Solvation in the Reaction of Hydrated (Di) electrons with Water to Create H2 and OH. *J. Chem. Theory Comput.* **2024**, *20*, 7337−7346.
(34) Gao, L.; Zhang, L.; Fu, Q.; Bu, Y. Molecular Dynamics Characterization of Dielectron Hydration in Liquid Water with Unique Double Proton Transfers. *J. Chem. Theory Comput.* **2021**, *17*, 666−677.
(35) Basco, N.; Kenney, G.; Walker, D. Formation and photodissociation of hydrated electron dimers. *Journal of the Chemical Society D: Chemical Communications* **1969**, 917−918.
(36) Peled, E.; Czapski, G. Molecular hydrogen formation (GH2) in the radiation chemistry of aqueous solutions. *J. Phys. Chem.* **1970**, *74*, 2903−2911.
(37) Basco, N.; Kenney-Wallace, G.; Vidyarthi, S.; Walker, D. A transient intermediate in the bimolecular reaction of hydrated electrons. *Can. J. Chem.* **1972**, *50*, 2059−2070.
(38) Buttersack, T.; Mason, P. E.; McMullen, R. S.; Schewe, H. C.; Martinek, T.; Brezina, K.; Crhan, M.; Gomez, A.; Hein, D.; Wartner, G.; et al. Photoelectron spectra of alkali metal−ammonia microjets: From blue electrolyte to bronze metal. *Science* **2020**, *368*, 1086−1091.
(39) Hartweg, S.; Barnes, J.; Yoder, B. L.; Garcia, G. A.; Nahon, L.; Miliordos, E.; Signorell, R. Solvated dielectrons from optical excitation: An effective source of low-energy electrons. *Science* **2023**, *380*, 1161−1165.
(40) Zurek, E.; Edwards, P. P.; Hoffmann, R. A molecular perspective on lithium−ammonia solutions. *Angew. Chem., Int. Ed.* **2009**, *48*, 8198−8232.
(41) Martyna, G. J.; Deng, Z.; Klein, M. L. Quantum simulation studies of singlet and triplet bipolarons in liquid ammonia. *J. Chem. Phys.* **1993**, *98*, 555−563.
(42) Mauksch, M.; Tsogoeva, S. B. Spin-paired solvated electron couples in alkali−ammonia systems. *Phys. Chem. Chem. Phys.* **2018**, *20*, 27740−27744.
(43) Zakharov, I. Quantum chemical DFT calculations of the local structure of the hydrated electron and dielectron. *Journal of Structural Chemistry* **2014**, *55*, 595−604.
(44) Luo, Q.; Zhang, C.; Bu, Y. Dielectron clathrate hydrates with unique superexchange spin couplings. *J. Phys. Chem. C* **2018**, *122*, 7635−7641.
(45) Kaukonen, H.-P.; Barnett, R.; Landman, U. Dielectrons in water clusters. *J. Chem. Phys.* **1992**, *97*, 1365−1377.
(46) Larsen, R. E.; Schwartz, B. J. Mixed quantum/classical molecular dynamics simulations of the hydrated dielectron: the role of exchange in condensed-phase structure, dynamics, and spectroscopy. *J. Phys. Chem. B* **2004**, *108*, 11760−11773.
(47) Larsen, R. E.; Schwartz, B. J. Full configuration interaction computer simulation study of the thermodynamic and kinetic stability of hydrated dielectrons. *J. Phys. Chem. B* **2006**, *110*, 1006−1014.
(48) Larsen, R. E.; Schwartz, B. J. Nonadiabatic Molecular Dynamics Simulations of Correlated Electrons in Solution. 2. A Prediction for the Observation of Hydrated Dielectrons with Pump- Probe Spectroscopy. *J. Phys. Chem. B* **2006**, *110*, 9692−9697.
(49) Barnett, R. N.; Giniger, R.; Cheshnovsky, O.; Landman, U. Dielectron Attachment and Hydrogen Evolution Reaction in Water Clusters. *J. Phys. Chem. A* **2011**, *115*, 7378−7391.
(50) De Grotthuss, C. Sur la décomposition de l'eau et des corps qu'elle tient en dissolution à l'aide de l'électricité galvanique. *Ann. chim* **1806**, *58*, 54.
(51) Agmon, N. The grotthuss mechanism. *Chem. Phys. Lett.* **1995**, *244*, 456−462.
(52) Perdew, J. P.; Ernzerhof, M.; Burke, K. Rationale for mixing exact exchange with density functional approximations. *J. Chem. Phys.* **1996**, *105*, 9982−9985.
(53) Grimme, S.; Antony, J.; Ehrlich, S.; Krieg, H. A consistent and accurate ab initio parametrization of density functional dispersion correction (DFT-D) for the 94 elements H-Pu. *J. Chem. Phys.* **2010**, *132*, 154104.
(54) Marzari, N.; Mostofi, A. A.; Yates, J. R.; Souza, I.; Vanderbilt, D. Maximally localized Wannier functions: Theory and applications. *Rev. Mod. Phys.* **2012**, *84*, 1419−1475.
(55) Hirata, S.; Head-Gordon, M. Time-dependent density functional theory within the Tamm−Dancoff approximation. *Chem. Phys. Lett.* **1999**, *314*, 291−299.
(56) Park, S. J.; Narvaez, W. A.; Schwartz, B. J. Ab initio studies of hydrated electron/cation contact pairs: Hydrated electrons simulated with density functional theory are too kosmotropic. *J. Phys. Chem. Lett.* **2023**, *14*, 559−566.
(57) Jou, F.-Y.; Freeman, G. R. Temperature and isotope effects on the shape of the optical absorption spectrum of solvated electrons in water. *J. Phys. Chem.* **1979**, *83*, 2383−2387.
(58) Carter-Fenk, K.; Mundy, C. J.; Herbert, J. M. Natural charge-transfer analysis: Eliminating spurious charge-transfer states in time-dependent density functional theory via diabatization, with application to projection-based embedding. *J. Chem. Theory Comput.* **2021**, *17*, 4195−4210.
(59) Campetella, M.; Maschietto, F.; Frisch, M. J.; Scalmani, G.; Ciofini, I.; Adamo, C. Charge transfer excitations in TDDFT: A ghost-hunter index. *J. Comput. Chem.* **2017**, *38*, 2151−2156.
(60) Jordan, C. J.; Coons, M. P.; Herbert, J. M.; Verlet, J. R. Spectroscopy and dynamics of the hydrated electron at the water/air interface. *nature communications* **2024**, *15*, 182.
(61) Martin, R. L. Natural transition orbitals. *J. Chem. Phys.* **2003**, *118*, 4775−4777.
(62) Migus, A.; Gauduel, Y.; Martin, J.; Antonetti, A. Excess electrons in liquid water: first evidence of a prehydrated state with femtosecond lifetime. *Physical review letters* **1987**, *58*, 1559.
(63) Long, F. H.; Lu, H.; Eisenthal, K. B. Femtosecond studies of the presolvated electron: an excited state of the solvated electron? *Physical review letters* **1990**, *64*, 1469.
(64) Savolainen, J.; Uhlig, F.; Ahmed, S.; Hamm, P.; Jungwirth, P. Direct observation of the collapse of the delocalized excess electron in water. *Nature Chem.* **2014**, *6*, 697−701.
(65) Hill, R. N. Proof that the H- ion has only one bound state. *Phys. Rev. Lett.* **1977**, *38*, 643.

https://doi.org/10.1021/acs.jpclett.4c02404
J. Phys. Chem. Lett. 2024, 15, 9557−9565

(66) Glover, W. J.; Larsen, R. E.; Schwartz, B. J. The roles of electronic exchange and correlation in charge-transfer-to-solvent dynamics: Many-electron nonadiabatic mixed quantum/classical simulations of photoexcited sodium anions in the condensed phase. *J. Chem. Phys.* **2008**, *129*, 164505.
(67) Pommeret, S.; Gobert, F.; Mostafavi, M.; Lampre, I.; Mialocq, J.-C. Femtochemistry of the hydrated electron at decimolar concentration. *J. Phys. Chem. A* **2001**, *105*, 11400−11406.
(68) Palianov, P.; Martin, P.; Quéré, F.; Pommeret, S. Ultrafast formation of hydrated electrons in water at high concentration: Experimental evidence of the free electron. *Journal of Experimental and Theoretical Physics* **2014**, *118*, 489−493.
(69) Abel, B.; Buck, U.; Sobolewski, A.; Domcke, W. On the nature and signatures of the solvated electron in water. *Phys. Chem. Chem. Phys.* **2012**, *14*, 22−34.
(70) Narvaez, W. A.; Wu, E. C.; Park, S. J.; Gomez, M.; Schwartz, B. J. Trap-seeking or trap-digging? Photoinjection of hydrated electrons into aqueous NaCl solutions. *J. Phys. Chem. Lett.* **2022**, *13*, 8653−8659.
(71) Stein, G. Photochemistry of the ferrocyanide ion in aqueous solution: hydrated electron formation and aquation. *Isr. J. Chem.* **1970**, *8*, 691−697.
(72) Christensen, H.; Sehested, K. The hydrated electron and its reactions at high temperatures. *J. Phys. Chem.* **1986**, *90*, 186−190.
(73) Kühne, T. D.; et al. CP2K: An electronic structure and molecular dynamics software package - Quickstep: Efficient and accurate electronic structure calculations. *J. Chem. Phys.* **2020**, *152*, 194103.
(74) Martyna, G. J.; Klein, M. L.; Tuckerman, M. Nosé−Hoover chains: The canonical ensemble via continuous dynamics. *J. Chem. Phys.* **1992**, *97*, 2635−2643.
(75) Goedecker, S.; Teter, M.; Hutter, J. Separable dual-space Gaussian pseudopotentials. *Phys. Rev. B* **1996**, *54*, 1703.
(76) Guidon, M.; Hutter, J.; VandeVondele, J. Auxiliary Density Matrix Methods for Hartree Fock Exchange Calculations. *J. Chem. Theory Comput.* **2010**, *6*, 2348−2364.
(77) Uhlig, F.; Herbert, J. M.; Coons, M. P.; Jungwirth, P. Optical spectroscopy of the bulk and interfacial hydrated electron from ab initio calculations. *J. Phys. Chem. A* **2014**, *118*, 7507−7515.
(78) Dreuw, A.; Weisman, J. L.; Head-Gordon, M. Long-range charge-transfer excited states in time-dependent density functional theory require non-local exchange. *J. Chem. Phys.* **2003**, *119*, 2943−2946.
(79) Dreuw, A.; Head-Gordon, M. Failure of Time-Dependent Density Functional Theory for Long-Range Charge-Transfer Excited States: The ZincbacteriochlorinBacteriochlorin and Bacteriochlorophyll Spheroidene Complexes. *J. Am. Chem. Soc.* **2004**, *126*, 4007−4016.
(80) Cline, J.; Takahashi, K.; Marin, T. W.; Jonah, C. D.; Bartels, D. M. Pulse Radiolysis of Supercritical Water. 1. Reactions between Hydrophobic and Anionic Species. *J. Phys. Chem. A* **2002**, *106*, 12260−12269.

https://doi.org/10.1021/acs.jpclett.4c02404
J. Phys. Chem. Lett. 2024, 15, 9557−9565